



HAL
open science

Targeting the endo-lysosomal autophagy pathway to treat inflammatory bowel diseases

Sruthi Vijaya Retnakumar, Ramasatyaveni Geesala, Alexis Bretin, Julien Tourneur-Marseille, Eric Ogier-Denis, Thorsten Maretzky, Hang Thi Thu Nguyen, Sylviane Muller

► **To cite this version:**

Sruthi Vijaya Retnakumar, Ramasatyaveni Geesala, Alexis Bretin, Julien Tourneur-Marseille, Eric Ogier-Denis, et al.. Targeting the endo-lysosomal autophagy pathway to treat inflammatory bowel diseases. *Journal of Autoimmunity*, 2022, 128, pp.1-11. 10.1016/j.jaut.2022.102814 . hal-03632352

HAL Id: hal-03632352

<https://hal.science/hal-03632352v1>

Submitted on 22 Jul 2024

HAL is a multi-disciplinary open access archive for the deposit and dissemination of scientific research documents, whether they are published or not. The documents may come from teaching and research institutions in France or abroad, or from public or private research centers.

L'archive ouverte pluridisciplinaire **HAL**, est destinée au dépôt et à la diffusion de documents scientifiques de niveau recherche, publiés ou non, émanant des établissements d'enseignement et de recherche français ou étrangers, des laboratoires publics ou privés.



Distributed under a Creative Commons Attribution - NonCommercial 4.0 International License

Targeting the endo-lysosomal autophagy pathway to treat inflammatory bowel diseases

Sruthi Vijaya Retnakumar^a, Ramasatyaveni Geesala^b, Alexis Bretin^{c,1}, Julien Tourneur-Marseille^d, Eric Ogier-Denis^e, Thorsten Maretzky^b, Hang Thi Thu Nguyen^c and Sylviane Muller^{a,f,g,*} 

^aCNRS and Strasbourg University, Unit Biotechnology and Cell signaling, UMR7242/ Strasbourg Drug Discovery and Development Institute (IMS), Strasbourg, France;

^bInflammation Program and Department of Internal Medicine, Roy J. and Lucille A. Carver College of Medicine, University of Iowa, Iowa City, IA, USA;

^cLaboratory M2iSH (Microbes, intestine, inflammation and Susceptibility of the host), UMR1071 Inserm, USC-2018 INRA, University of Clermont Auvergne, Clermont-Ferrand, France;


^dCentre de recherche sur l'inflammation, UMR1149 Inserm, Université de Paris, Paris, France;

^eLaboratory COSS (Chemistry, Oncogenesis, Stress Signaling), UMR1242 Inserm, Université de Rennes-1/ Centre de Lutte contre le Cancer CLCC Eugène Marquis, Rennes, France;

^fFédération Hospitalo-Universitaire (FHU) OMICARE, Fédération de Médecine Translationnelle de Strasbourg (FMTS), Strasbourg University, Strasbourg, France;

^gUniversity of Strasbourg Institute for Advanced Study (USIAS), Strasbourg, France.

*Corresponding author. CNRS/Université de Strasbourg UMR7242 Biotechnologie et Signalisation Cellulaire, Institut de science et d'ingénierie supramoléculaires, 8 Allée Gaspard Monge, 67000 Strasbourg, France. *Email address*: sylviane.muller@unistra.fr (S. Muller).

ORCID  S. Muller: 0000-0002-0481-0620

Email addresses of coauthors

Sruthi Vijaya Retnakumar: sruthi.vijaya-retnakumar@etu.unistra.fr

Ramasatyaveni Geesala: rageesal@utmb.edu

Alexis Bretin: abretin@gsu.edu

Julien Tourneur-Marseille: julien.tourneur-marseille@inserm.fr

Eric Ogier-Denis: eric.ogier-denis@inserm.fr

Thorsten Maretzky: thorsten-maretzky@uiowa.edu

Hang Thi Thu Nguyen: hang.nguyen@uca.fr

Sylviane Muller : sylviane.muller@unistra.fr

¹Present address: Center for Inflammation, Immunity, and Infection, Institute for Biomedical Sciences, Georgia State University, Atlanta, GA, 30303, USA

ABSTRACT

Inflammatory bowel disease (IBD) is a serious public health problem in Western society with a continuing increase in incidence worldwide. Safe, targeted medicines for IBD are not yet available. Autophagy, a vital process implicated in normal cell homeostasis, provides a potential point of entry for the treatment of IBDs, as several autophagy-related genes are associated with IBD risk. We conducted a series of experiments in three distinct mouse models of colitis to test the effectiveness of therapeutic P140, a phosphopeptide that corrects autophagy dysfunctions in other autoimmune and inflammatory diseases. Colitis was experimentally induced in mice by administering dextran sodium sulfate and 2,4,6 trinitrobenzene sulfonic acid. Transgenic mice lacking both *il-10* and *iRhom2* – involved in tumor necrosis factor α secretion – were also used. In the three models investigated, P140 treatment attenuated the clinical and histological severity of colitis. Post-treatment, altered expression of several macroautophagy and chaperone-mediated autophagy markers, and of pro-inflammatory mediators was corrected. Our results demonstrate that therapeutic intervention with an autophagy modulator improves colitis in animal models. These findings highlight the potential of therapeutic peptide P140 for use in the treatment of IBD.

Keywords

Inflammatory bowel diseases • Colitis • Murine models • Autophagy • Peptide-based treatment

1. Introduction

IBD is a public health challenge with a high incidence in Western countries, but is also increasing sharply in newly-industrialized countries. Crohn's disease (CD) and ulcerative colitis (UC), the main forms of inflammatory bowel disease (IBD), were the first chronic disorders in which autophagy dysfunctions were suggested to play a potentially major etiopathogenic role [1,2]. Population-based studies provide compelling evidence that genetic factors contribute to the pathogenesis of IBD, and many IBD risk loci have been identified. However, IBD has multifactorial triggers, including genetic, microbial, and environmental factors, causing dysregulation of the innate and adaptive immune system in the intestine [3–6].

IBD has high recurrence, and low cure rates [7], and we currently lack effective treatment options, primarily due to either limited efficacy or unsustainable side effects [8–10]. Today, therapies are largely limited to treatment of symptoms with the aim of improving the patient's quality of life. However, even with this limited scope, the effectiveness of treatment varies dramatically between patients [11–13]. More ambitious therapies, including cytokine blockers, such as therapeutic monoclonal antibodies (mAb) adalimumab and infliximab, directed against tumor necrosis factor-alpha (TNF- α), or ustekinumab, targeting interleukin (IL)-12 and IL-23, were recently tested in patients with severe, active CD [14]. Therapeutic mAbs targeting integrins (*e.g.*, vedolizumab, natalizumab) have also been tested. All these treatments produce heterogeneous patient responses [11], added to which, their cost and high potential for serious toxicity limit their long-term clinical use. Strategies based on small molecules, such as molecules in the Janus kinase (JAK) pathway, have also been explored, and numerous compounds, including herbal extracts are under clinical evaluation, alone or in combination [15,16]. Many have only shown limited effectiveness to date [9,10,17,18].

P140 is a 21-mer phosphopeptide derived from the cognate sequence 131-151 of the U1-70K spliceosomal protein [19]. It contains a phosphoserine residue at position 140 that is inserted during synthesis. Using lysosomes purified from the liver of untreated or P140-treated MRL/lpr lupus-prone mice, we previously showed that P140 regulates chaperone-mediated autophagy (CMA) – a process that contributes to degradation of intracellular proteins in lysosomes – at the lysosomal substrate uptake step [20]. P140 downregulates hyperactive autophagy processes and (probably as a direct consequence) decreases expression of major histocompatibility complex-II molecules, which is relevant in its action on lupus [20–22]. P140 has since been shown to be effective in murine models of primary and secondary Sjögren's

syndrome [23,24], chronic inflammatory demyelinating polyneuropathy [25], and chronic house dust mite-induced airway inflammation [26].

The potential of P140 in the IBD context is based on its targeting of autophagy. Indeed, in addition to barrier functions and immune responses, numerous risk loci for IBD are situated in regions containing genes encoding proteins involved in autophagy [5,27–30]. Specifically, polymorphisms in autophagy-related (Atg) genes, such as *ATG16L1*, sequestosome (*SQSTM1*)/p62, serine/threonine-protein kinase *ULK1*, immunity-related GTPase M (*IRGM*), nucleotide-binding oligomerization domain 2 (*NOD2*)/*CARD15* are associated with an increased risk of developing CD [1,31–36] or IBD [8,37]. Functional studies [5] have emphasized the pivotal role played by dysfunctional autophagy in intestinal homeostasis functions, leading to pathogenic hallmarks of IBD. Autophagy was found to be indispensable in the maintenance of intestinal epithelial barrier integrity by protecting intestinal epithelial cells against TNF-induced apoptosis [38,39] or *via* the degradation of tight junction barrier proteins such as Claudin-2 [40]. Paneth and goblet cells are specialised cell types of the intestinal epithelium involved in the secretion of antimicrobial peptides and mucins, respectively, to protect against pathogenic microbes; autophagy deficiency in these cells severely impacts their secretory functions [41,42]. In addition, the loss of autophagy in immune cells has been associated with elevated inflammasome activation [43] as well as impaired antigen presentation responses against pathogens [44] and therefore an increased susceptibility to colitis. Various studies have also demonstrated that autophagy dysfunctions lead to altered gut microbial composition or gut dysbiosis [45,46]. We hypothesized that P140 could correct these defects, reducing the extent of molecular and cellular inflammation, and could delay the development of the disease.

We, therefore, evaluated the effectiveness of P140 in three distinct but complementary murine models of colitis – two chemically-induced models, and one that spontaneously develops chronic intestinal inflammation with UC-like features due to a double mutation in *il-10* and *rhomboid 2* (iRhom2) genes [47]. Analysis of these three independent models revealed that treatment with P140 attenuates inflammation and disease at the clinical and histological levels. Expression levels for several pro-inflammatory mediators were significantly diminished in colonic tissues. Mechanistically, we found that P140 corrected autophagy defects in the target tissues (colon) and spleens from mice with colitis.

2. Methods

2.1. Peptides

P140 (RIHMOVYSKRpSGKPRGYAFIEY) and Sc140 (YVSRYFGpSAIRHEPKMKIYR) phosphopeptide (where pS represents phosphoserine residues) were synthesized using classical N-[9-fluorenyl] methoxycarbonyl solid-phase chemistry, and purified by reversed-phase high-performance liquid chromatography (RP-HPLC) [19,48]. Peptide homogeneity was checked by analytical HPLC, and their identity was assessed by liquid chromatography-mass spectrometry (LC-MS) on a Finnigan LCQ Advantage Max system (Thermo Fischer Scientific, Courtaboeuf, France).

2.2. Mouse models of colitis

Three independent experiments (A, B, C) were performed in the DSS model with distinct protocols (**Figure 1**). Following these experiments, mice were sacrificed by exsanguination through direct cardiac puncture under isoflurane anesthesia. All mice were housed under specific pathogen-free conditions in the respective animal care facilities. Mice were weighed daily, and stool consistency, diarrhea, or blood in the stools were monitored to calculate the disease activity index (DAI).

In Exp. A, 7-week-old C57BL/6 male mice (Charles River Laboratories, France) were induced with DSS from day 0 (2.0% w/v; MP Biomedicals 160110 added to the animals' drinking water). They were treated with either P140 (4 mg/kg mouse body-weight, intravenously (i.v.)) or vehicle (NaCl) on days -2 and -1, and then at days +2, +5 and +7 (preventive and curative experimental design). The control peptide ScP140 was not administered in this experiment. Mice were sacrificed on day +9.

In Exp. B, 8-week-old C57BL/6 female mice (Japan SLC, Japan) received 2.5% w/v DSS (MP Biomedicals) for 5 days [49]. They were treated with P140 and ScP140 peptides (i.v.) on days 0 and +2, and sacrificed on day +5. A group of DSS-induced mice was also treated orally with 100 mg/kg mesalazine (Kobayashi Kako) once daily for 4 days (day 0 to day +4). Total volume of mesalazine: 10 mL/kg in 0.5% w/v carboxymethyl cellulose [50].

In Exp. C, 6-week-old C57BL/6 male mice (Janvier Laboratories, France) received 2.0% w/v DSS (MP Biomedicals) for 7 days (replaced by sterile water on day +7). Peptides were administered i.v. in curative mode, every two days from day +7 to day +14, and mice were sacrificed on day +21.

Two distinct protocols (D, E) were evaluated with the TNBS model (**Figure 1**). In Exp. D, 8-week-old BALB/c female mice (Janvier Laboratories) maintained in standard cages and fed

with classic standard chow and tap water *ad libitum*, received TNBS (Sigma-Aldrich, 2508-19-2; 100 mg/kg mouse body-weight) intrarectally (i.r.) on day 0 (instillation of 50 μ L 50% v/v ethanol under anesthesia with 3% isoflurane *via* nose cone). P140, ScP140, or vehicle were administered i.v. on days +1, +3 and +5. Control mice received an intrarectal instillation of 50 μ L 50% ethanol. As above, clinical parameters were monitored daily. Mice were sacrificed on day +8 by isoflurane overdose followed by cervical dislocation.

Exp. E included C57BL/6 mice - less susceptible to TNBS than BALB/c mice [51]. Eight-week-old male mice (Charles River laboratories, France) were anesthetized with a subcutaneous injection of xylazine/ketamine, and TNBS (Sigma-Aldrich, 92822) dissolved in 50% ethanol (40 μ L) was administered intrarectally at 150 mg/kg mouse body-weight. Control mice received an intrarectal instillation of 40 μ L 50% ethanol. Mice were treated i.v. with P140, ScP140, or vehicle on days +1, +2 and +3 (4 mg peptide/kg body-weight). Animals were sacrificed on day +4 by cervical dislocation.

il10^{-/-}/iRhom2^{-/-} mice [47] were used as a genetic model of IBD in Exp. F. P140 therapy was initiated at 8 weeks of age (onset of the disease in these mice). P140, ScP140 (both at 100 μ g peptide/mouse), or vehicle was administered i.v. twice a week for 11 weeks. Mice were sacrificed 11 weeks after initiating treatment.

The scores used to evaluate the disease intensity are described in **Supplementary Tables 1 and 2**. At the time of sacrifice, the gastrointestinal tract was collected and weighed, opened longitudinally, and washed several times according to standard procedures. Colon sections were isolated as shown in **Supplementary Figure 1**.

2.3. *Histological analysis*

Colons were immediately fixed in 4% w/v paraformaldehyde and embedded in paraffin. 5-mm-thick tissue sections were stained with hematoxylin and eosin (H&E) and observed under a light microscope. Histological damage was assessed based on the criteria described in **Supplementary Table 3**.

2.4. *Immunofluorescence*

Paraffin-embedded colonic tissues were cut into 7-mm-thick sections. Non-specific binding was blocked with phosphate-buffered saline containing 5% w/v bovine serum albumin and 0.2% Tween-20. Primary antibodies were incubated at 4 °C overnight and the corresponding secondary antibodies at room temperature for 4 h. The following antibodies were

used: SQSTM1/p62 (Abcam, ab109012), Alexa Fluor 488 goat anti-rabbit IgG (H+L) cross-adsorbed secondary antibody (Invitrogen, A-11008). Nuclei were labeled with Hoechst 33258 (Invitrogen, H1398). Slides were mounted with Fluoromount-G (ThermoFisher Scientific, 00-4958-02). Confocal (Carl Zeiss) images were acquired, and fluorescence intensity was measured using Fiji software.

2.5. *Western blotting*

Autophagy protein expression was measured in colon or spleen tissue homogenates by western blotting, as described [25,52]. Antibodies were: MAP1LC3B (Novus Biologicals, NB100-2220), SQSTM1/p62 (Abcam, ab109012), BECLIN1/BECN1 (Abcam, ab207612), ATG5 (Cell Signaling Technology, 12994S), lysosomal-associated membrane protein (LAMP)2A (Abcam, ab18528), and HSPA8 (Abcam, ab51052), HSP90 (Abcam, ab203126). Secondary antibodies were horseradish peroxidase-conjugated goat anti-mouse or anti-rabbit IgG antibody (Jackson ImmunoResearch, 115-035-008 and 111-035-008; 50 ng/mL). Signal was detected using Clarity western ECL Substrate (Bio-Rad, 1705061). Expression levels of autophagy markers were normalized by densitometry relative to the total protein level, using Image Lab (Bio-Rad) software.

2.6. *MPO activity assay*

Granulocyte infiltration into the colon was quantified by measuring MPO activity. Briefly, selected colon sections (**Supplementary Figure 1**) were homogenized using a Mixer Mill MM 400 (Retsch) and resuspended in 50 mM phosphate buffer (pH 6.0) containing 0.5% hexadecyltrimethyl ammonium bromide (Sigma-Aldrich, 57-09-0; 50 mg/mL). The homogenate was sonicated for 10 s and centrifuged at 13,400 x g for 6 min. An aliquot (25 μ L) of supernatant was used for the assay following appropriate dilution. The final reaction was visualized by adding H₂O₂ as peroxidase substrate and 3,3',5,5'-tetramethylbenzidine as chromogen, and incubating for 30 min at 37 °C. The reaction was blocked by the addition of 1 M HCl, before measuring absorbance at 450 nm using a plate reader (Thermo Scientific Multiskan GO). Results were expressed as absorbance per mg of tissue.

2.7. *qRT-PCR*

Total RNA was extracted using the NucleoSpin RNA isolation kit (Macherey Nagel, 740955.250) from a portion of colon (**Supplementary Figure 1**) following homogenization in

a Mixer Mill MM 400 (Retsch). RNA was reverse-transcribed using the iScript gDNA Clear cDNA Synthesis Kit (Bio-Rad, 172-5035). qRT-PCR was performed using Sso Advanced Universal SYBR Green Supermix (Bio-Rad, 172-5274) with the CFX C1000 Touch™ Real-Time PCR detection system (Bio-Rad, 1855195). Primers used are listed in **Supplementary Table 4**. A GeNorm study was performed using Bio-Rad's CFX Maestro 1.1 software with ten housekeeping genes (*Actb*, *B2m*, *G6pd*, *Gusb*, *Hprt1*, *Rpl13a*, *Rps18*, *Taf8*, *Tfrc*, *Ywhaz*), to determine which were the most stable in our conditions. The three most stable, or acidic ribosomal phosphoprotein P0 (*36b4*) in some experiments, were used for data normalization. Data were analyzed by the $\Delta\Delta C_T$ method, as follows: $\Delta\Delta C_T = (C_{T, target} - C_{T, reference})_{test} - (C_{T, target} - C_{T, reference})_{calibrator}$, and the final data were derived from $2^{-\Delta\Delta C_T}$.

2.8. *Ex-vivo* colon culture and ELISA-based cytokine quantification

Segments of the distal colon (0.5 cm-long; **Supplementary Figure 1**) were dissected and washed in PBS containing penicillin and streptomycin. Segments were then placed in 24-well flat-bottomed culture plates containing 500 μ L complete RPMI 1640 medium and incubated at 37 °C under 5% CO₂ for 24 h. Culture supernatants were harvested and assayed for keratinocyte-derived chemokines [53] using a commercial ELISA kit (KC/CXCL1; Mouse CXCL1/KC DuoSet ELISA, DY453, R&D Systems). Serum samples prepared from blood samples collected at the time of sacrifice were also assayed for cytokines/chemokines – IL-6 (DY406-05), IFN-gamma (DY485-05), IL-12 p70 (DY419-05), TNF- α (DY410-05), and IL-1 β (DY401-05) – using commercial kits (R&D systems) according to the supplier's protocols. Standard curves were generated by titration with recombinant protein calibrators provided in commercial kits.

2.9. Statistical analysis

All values are expressed as mean \pm SEM. Statistical analyses were performed using GraphPad Prism (Version 8.0). Statistics are described in the corresponding figure legends. *P* values \leq 0.05 were considered statistically significant.

2.10. Ethics statement

Experiment protocols involving animals were approved by the local Institutional Animal Care and Use Committee and the French ministry for higher education, research and innovation (APAFIS #20654-2019061116549343; APAFIS #2171-2019092716434837; APAFIS #26681-

2020072115122312). In line with these agreements, and taking into account the best European practices in the field (3-R rules), we took the necessary measures to avoid pain and minimize distress and pointless suffering of mice during experiments and at the time of sacrifice. Animals were maintained under controlled environmental conditions (20 ± 2 °C) in either specific pathogen-free or conventional husbandry conditions (as specified above). A 12 h/12 h light-dark cycle (lighting 7:00 a.m.-7:00 p.m.) was maintained. Mice were housed in large polycarbonate cages, with 8 to 10 mice per cage on bedding made from spruce wood chips (Safe) and enriched with play tunnels which were changed weekly. Mice monitored in Japan (Exp. B) were housed and cared for in accordance with the Japanese Pharmacological Society Guidelines for Animal use. Animals (a maximum of 4 per cage; TPX cages, CLEA Japan) were maintained under controlled environmental conditions of temperature (23 ± 3 °C), humidity ($50 \pm 20\%$), and lighting (8:00 a.m.-8:00 p.m.). Experiments with *il10^{-/-}/iRhom2^{-/-}* mice (Exp. F) were conducted according to the institutional regulations for animal care and use of the University of Iowa.

3. Results

3.1. *The autophagy modulator P140 ameliorates disease progression in three murine models of colitis*

We first investigated the effect of P140 in a mouse model of dextran sodium sulfate (DSS)-induced colitis. In the three DSS protocols tested (**Figure 1**; Exp. A, B, C), mice developed colitis, as indicated by the clinical parameters measured (**Figure 2**; **Supplementary Figures 2 and 3**). No effect was observed in Exp. B (mesalazine that is commonly used to treat patients with IBD, was also inactive) or Exp. C (**Figure 2 and Supplementary Figures 2 and 3**). However, beneficial clinical effects of P140 were observed in Exp. A, where P140 was administered according to both preventive and curative protocols, P140-treated mice had longer colons, less blood in stools, and decreased DAI scores (**Figure 2 A-C**).

To further examine the curative potential of P140, we used another chemically-induced colitis model, the widely used 2,4,6-trinitrobenzene sulfonic acid (TNBS) mouse model. TNBS-induced mice developed colitis in the two protocols evaluated (Exp. D, E) (**Figure 3**; **Supplementary Figure 4**). In Exp. D, P140 did not significantly improve any of the clinical and biochemical parameters assessed (**Supplementary Figure 4**). In Exp. E, although not significant, a trend for decreased mortality (with unexplained weight loss; **Figure 3A**) was observed in the group of mice treated with P140 (13% mortality *versus* 39% of TNBS-induced

mice treated with vehicle, and 40% of TNBS-induced mice treated with a scrambled (Sc) analogue of the P140 sequence; **Figure 3B**). This effect was associated with improvement to colonic lesions at macroscopic and histological levels. Thus, P140 decreased the extent of inflammatory lesions by 35% according to the Wallace score, compared to only 15% in mice that received ScP140 (**Figure 3C**). The Ameho score (grading on a scale from 0 to 6) – which considers the degree of the inflammatory infiltrate, the presence of erosion, ulceration or necrosis, and the depth and surface extension of the lesions – was decreased by 41% in the P140 group (3.13 ± 0.63 versus 5.28 ± 0.41 in vehicle-treated TNBS-induced mice; **Figure 3D**). Surprisingly, in this experiment, ScP140 also reduced inflammation in TNBS-induced mice, although less efficiently (Ameho scores = 3.67 ± 0.78 , corresponding to a 31% improvement of inflammatory lesions).

As part of our analysis of inflammation, we also evaluated myeloperoxidase (MPO) activity. MPO is one of the best diagnostic biomarkers of inflammation and oxidative stress. This ancestor of cyclooxygenase helps to defend gut-associated lymphoid tissue against harmful enteric microbes, while tolerating harmless commensal bacteria and dietary antigens. MPO activity correlates with the severity of experimentally-induced colitis [54]. Activity of this enzyme in mice with TNBS-induced colitis was significantly reduced following P140 treatment compared to vehicle- or ScP140-treatment (**Figure 3E**).

In the experiments described above, no sign of toxicity of P140 peptide was noticed, even under inflammatory conditions. Changes in body-weight can be used as an indirect marker of colonic lesions in mice with chronic colitis [55]. Although we studied acute colitis, this parameter was used to demonstrate homogeneity of groups before its induction, and to detect possible toxic effects of the treatments tested. Therefore, animals were weighed before inducing colitis and daily until sacrifice. No change in body weight with regard to the control groups was observed following treatment with P140 (4 mg/kg mouse body-weight for each injection in Exp. A-E) (see **Figure 3B**; **Supplementary Figures 2A, 3A, 3C, 4B**).

In addition to the chemically-induced models, we also evaluated the effect of P140 in a genetic model of spontaneous IBD (Exp. F; **Figure 4**). Mice lacking both *il10* and *iRhom2* (*il10*^{-/-}*iRhom2*^{-/-}) develop early intestinal inflammation followed by accelerated weight loss within 8 to 12 weeks of birth [47]. Using this novel mouse model, we extended our findings from the chemically-induced colitis models. At 6-8 weeks of age (onset of the disease), mice received either P140 or ScP140 twice per week for 10 weeks (**Figure 4A**). Mortality was significantly decreased in the group of mice treated with P140, as compared to the ScP140 group and the group of *il10*^{-/-}*iRhom2*^{-/-} mice let untreated (**Figure 4B**). P140-treated mice also

showed improved weight gain (**Figure 4C**) and reduced colon inflammation, as reflected by an increase in colon length (**Figures 4D, 4E**). In addition, the size and weight of spleens from P140-treated mice were significantly decreased **with regard to the two other groups of mice used as controls** (**Figures 4F**).

As the onset of colitis is strongly linked to inflammation and defects in autophagy, we next investigated the effect of P140 on these processes.

3.2. P140 treatment reduces the production of several pro-inflammatory mediators in colons from DSS-induced mice

Compared to mice with DSS-induced colitis treated with vehicle only, several genes involved in inflammation were significantly down-regulated in colons collected from mice treated with P140 (**Figure 5; Supplementary Figure 5; Exp. A**). These genes included *Tnfa*, *Il6*, *Kc/Cxcl1*, *Mcp1/Ccl2* and *Il12a*. The level of secreted KC/CXCL1 protein remained unchanged in colon culture supernatants, as measured by ELISA (**Supplementary Figure 5F**). No change in *Il1 β* , *Inf γ* , *Il-17a*, *Gm-csf* and *Mip2* gene expression was detected (**Supplementary Figure 5A-E**). Following P140 treatment, no change in gene expression levels was detected in colon tissues from mice with TNBS-induced colitis in Exp. E (**Supplementary Figure 6**), and circulating cytokine levels were below the sensitivity limit of the commercial ELISA kits used.

3.3. Autophagy processes are defective in colons from mice with colitis and are partially corrected by P140 peptide

The mRNA and protein expression levels of a series of markers characteristic of macroautophagy and CMA were evaluated by quantitative reverse transcription PCR (mRNA) and western blot (protein). In terms of gene expression, no change was observed for several of them – including *Sqstm1*, *Lamp2*, or (at the limit of significance) *Map1lc3b* – in colon cells from mice with DSS-induced colitis. However, a statistically significant decrease was detected for others (*Mtor*, *Ulk1*, *Becn1*, *Atg14*, *Atg5*, *Atg12*, and *Atg16l1*). The altered expression of *Atg14*, *Atg5* and *Map1lc3b* was clearly compensated following treatment with P140 (**Supplementary Figures 7D, 7E, 7H**).

At the protein level, in Exp. A, equivalent levels of ATG5-ATG12, MAP1LC3BII/I, BECN1, HSPA8, and HSP90 were measured in DSS-induced and control (healthy) mice. SQSTM1 and LAMP2A expression was increased in DSS-induced mice, but was corrected by

P140 treatment (**Figures 5H, 5I; Supplementary Figure 8**). Results from Exp. B were less conclusive, with similar levels of protein markers ATG5-ATG12 and BECN1, but also SQSTM1, and LAMP2A detected in colon tissues from DSS-induced and healthy mice. In this experiment, expression of MAP1LC3BII/I and HSPA8 decreased upon exposure to DSS, but no compensation was observed following treatment with P140.

In colon tissues from TNBS-induced mice (Exp. E), no change in ATG5/12, BECN1, MAP1LC3B, SQSTM1, HSPA8, HSP90, or LAMP2A protein expression was detected. We also had access to spleens from these animals. Once again, expression levels for ATG5/12, SQSTM1, HSPA8, and LAMP2A were equivalent in TNBS-induced and healthy mice. However, a trend for an increasing ratio between cytosolic MAP1LC3B-I and autophagosome membrane-bound MAP1LC3B-II (MAP1LC3B puncta) –indicating active autophagy – was observed in mice with colitis (**Figures 3F, 3G**), and corrected upon treatment with P140, with a return to the basal ratio (**Figure 3G**). No significant effect was observed with the control peptide ScP140.

4. Discussion

The aim of this study was to determine whether the phosphopeptide P140, which has been shown to influence autophagy linked to several human diseases, could have a positive impact on IBD.

Using two chemically-induced mouse models of colitis and a genetic model that spontaneously develops early intestinal inflammation, we demonstrated for the first time the protective potential of P140 in an intestinal inflammatory disorder. In the three murine models evaluated, P140 treatment attenuated the clinical and histological severity of colitis and, in the DSS-induced model, expression levels for several pro-inflammatory mediators were decreased. From a mechanistic point of view, our results confirmed that – as in MRL/lpr lupus-prone mice, where the mode of action of P140 was initially identified [20–22] – P140 affected macroautophagy and CMA in colon cells and splenocytes from mice with colitis, as indicated by decreased expression of biomarkers.

The chemically-induced models of colitis selected for this investigation are commonly used to assess the efficacy of candidate pharmacological treatments. DSS is a chemical colitogenic with anticoagulant properties. It causes epithelial cell death, leading to compromised intestinal barrier function and inflammation [50,55,56]. TNBS promotes transmural colitis with severe diarrhea, weight loss, and rectal prolapse, as found in patients with CD [57,58]. The genetic

model of colitis was important in this investigation due to its clinical relevance, particularly as it allows long-term study. IL-10 plays a key role in both innate and adaptive immunity, through its regulation of inflammatory responses in the intestine. A small proportion (5%) of mice lacking IL-10 spontaneously develop colitis at 2-8 months of age. Disease onset can be accelerated by exposing mice to piroxicam, a nonsteroidal anti-inflammatory drug in the oxicam class. Histologically, colitis in *il10*^{-/-} mice is similar to human IBD [59]. iRhom2 is a crucial regulator of TNF α secretion in myeloid cells. Recently, we reported that mice lacking both iRhom2 and IL10 developed severe colitis [47] at 8 weeks of age, with significantly increased colonic inflammation, gut dysbiosis and permeability.

The use of several distinct experimental mouse models strengthens the results presented here. Indeed, IBD is particularly difficult to study as models can be inconsistent, potentially presenting a high degree of variability from one experiment to another. This variability is linked to several parameters, *e.g.*, the method used to induce colitis, doses administered and duration (acute or chronic model), the sex and strain of mice used, the conditions in which animals are housed. In addition, due to the severity of the disease and the associated pain, it is often necessary to limit the period over which animals are observed [50,57]. In addition to the different models, various induction designs (strain and sex of experimental animals, concentration of inducer, duration of the experiment until sacrifice) and treatment protocols (number of injections, timeframe between peptide doses) were tested to fully explore the efficacy of P140, delivered via the route validated previously in several studies of inflammation [21,23–26].

In terms of the course of disease progression, our results show a clear favorable outcome following P140 treatment. Curative therapy was applied with the TNBS model; both prophylactic and curative treatments were used with the DSS model; and *il10*^{-/-}/*iRhom2*^{-/-} mice were successfully treated preventively for 10 weeks. Translation to patients will require additional studies to precisely determine the optimal conditions for use, including prevention, but also treatment of established IBD conditions as part of disease control.

Through its disruption of the intestinal epithelial barrier, DSS allows entry of luminal bacteria or bacterial antigens into the mucosa, leading to enterocolitis [50,55,56]. Inflammation is known to be involved in the pathogenesis of IBDs, including through the recruitment (migration and infiltration) of monocytes/macrophages to inflamed intestinal tissues. Following P140 treatment, inflammation was significantly reduced in colonic mucosa from DSS-induced mice. In TNBS-induced mice, where an excessive cell-mediated immune response involving acute Th1 inflammation develops, P140 treatment reduced macroscopic and colon damage

scores, as well as excessive MPO activity. In this model, no visible effect of P140 on cytokine/chemokine production was observed. Differences in cytokine levels between the two colitis models have also been reported and discussed elsewhere [60–62]. However, this result could also be linked to the duration of the experiment (4 days), or the fact that several mice in this group died before the end of the experiment, and consequently tissue samples were unavailable.

In support of our results, orally-administered 5-aminosalicylic acid compounds such as mesalazine or olsalazine, as well as the corticosteroid budesonide have been reported to display limited efficacy in DSS-induced mice [50]. This lack of effect seems to be related to the pharmacokinetics and metabolism of these compounds, and their capacity to reach inflamed colon tissues before being metabolized in the liver.

Dysfunctional autophagy has been reported in intestinal biopsies from IBD patients, and other mouse models [5,63], and an important result from this investigation was the demonstration that autophagy is dysfunctional in colon cells and splenocytes from mice with colitis, and the evidence that it could be at least partially restored by P140. The autophagic flux is classically used to represent the dynamic process of autophagy, but due to the experiment design, we were unable to assess its intensity. In the two chemically-induced models of colitis used here, compared to control mice, several key autophagy markers were expressed at equivalent levels. These results could be due to experimental parameters, in particular the timing of tissue sampling, and/or to inherent difficulties detecting autophagy markers in colon tissues (as highlighted by Klionsky et al. [64]). However, since colon samples were isolated following a precisely established dissection procedure, we are confident that biases were avoided.

In DSS-induced mice, the expression of other autophagy markers, including ATG14, ATG5, and ATG12 (mRNA level; decrease), as well as SQSTM1 and LAMP2A (protein level; increase), was altered.

SQSTM1 is a classical autophagic cargo adaptor which can itself become degraded during the autophagy process. Accumulation of this protein suggests that autophagy is either decreased or inhibited in DSS-induced colitis. As SQSTM1 transcription is known to be sensitive to many factors, including prolonged starvation and endoplasmic reticulum stress, it is important to verify its mRNA levels if its protein level is used as an indicator of autophagy [65]. We found no change in SQSTM1 transcript levels in mice with colitis. Increased accumulation of SQSTM1 protein combined with a decrease in ATG14, ATG5, and ATG12 transcription, suggests dysfunctional autophagy in the intestines of DSS-induced mice – like that observed in

patients – P140 treatment restored basal expression levels for all five markers identified, suggesting that autophagy had recovered.

The functional role played by CMA is relatively poorly understood in IBD. LAMP2A acts as the receptor for CMA substrates at the lysosomal membrane, and determines the rate of CMA activity. In patients with colorectal cancer, increased LAMP2A expression has been described to promote proliferation of cancer cells [66]. The increased LAMP2A (protein) level observed here could reflect an increase in CMA activity in the colon of DSS-induced mice. Except in some specific circumstances such as oxidative stress, the lysosomal level of LAMP2A is regulated by decreasing its degradation rate, with transcription remaining stable [67]. As we only measured total LAMP2 transcription, we cannot conclude that there was no change in transcription of the LAMP2A isoform.

BECN1 plays a critical role in regulating autophagy, and is also involved in tumor and metastasis formation, particularly in colorectal cancer, through an autophagy-independent pathway [68]. BECN1 protein expression was unchanged here, despite a moderate decrease in its mRNA expression. However, autophagy-dependent phosphorylation of BECN1 is strongly dependent on ATG14, which promotes BECN1 translocation from the trans-Golgi network to autophagosomes while also enhancing phosphatidylinositol 3-kinase catalytic subunit type 3 activity in a BECN1-dependent manner [69]. ATG14 is therefore pivotal in autophagosome-endolysosome fusion [70]. Expression of ATG14 was strongly reduced in colon cells from DSS-induced mice.

5. Conclusions

In conclusion, our results show that P140 alleviates colitis in murine models, as characterized by decreased DAI or clinical and histological scores, reduced colon shortening, lower levels of MPO activity, and down-regulated pathogenic cytokine and chemokine expression in colonic mucosa. In the patho-physiologically relevant tissues (colon cells), P140 regulated markers of both macroautophagy (ATG14, ATG5, ATG12, SQSTM1) and CMA (LAMP2A), suggesting that as shown in lupus, it might affect both upstream and downstream elements of the endo-lysosomal autophagy pathway. The molecular mechanisms through which P140 controls autophagy in IBD will need to be further investigated, and head-to-head trials with drugs that are currently used to treat patients with IBDs or other proposed treatments [10,50,71–73] should be performed. Nevertheless, our results strongly suggest that the phosphopeptide P140 – which has been demonstrated to be safe in clinical trials involving

patients with SLE [74,75] – could also be used, alone or in combination with other medication [15,16,63,76,77], to treat patients with IBD, either preventively, or as part of disease control.

Author Contributions

SM, TM, and HN designed the experiments. SVR, RG, JTM, and HN performed experiments. SVR, RG, TM, HN, and SM analyzed the results. SM wrote the paper. All authors approved the manuscript.

Declaration of competing interest

SM is named as co-inventor on CNRS-ImmuPharma patents relating to P140 peptide. TM holds a patent on a method to identify agents for use in combination with inhibitors of iRhoms. The other authors have no potential conflicts of interest to disclose. All the authors declare that the research was conducted in the absence of any commercial or financial relationships that could be construed as a potential conflict of interest.

Acknowledgments

We thank Dominique Ciocca for assistance with animal colony management and animal handling.

Funding

SM was funded by the French Centre National de la Recherche Scientifique (CNRS), Région Grand-Est, and the Laboratory of Excellence Medalis (ANR-10-LABX-0034). This work was undertaken at the Interdisciplinary Thematic Institute IMS, as part of the ITI 2021-2028 program of the University of Strasbourg, CNRS and Inserm, and received further support from IdEx Unistra (ANR-10-IDEX-0002) and SFRI (STRAT'US project, ANR-20-SFRI-0012) in the framework of the French Investments for the Future Program. SM also acknowledges support from the University of Strasbourg Institute for Advanced Study (USIAS), the TRANSAUTOPHAGY COST Action (CA15138), the Club francophone de l'autophagie (CFATG), the European Regional Development Fund of the European Union in the framework of the INTERREG V Upper Rhine program, and ImmuPharma-France. **HN** was funded by the Ministère de la Recherche et de la Technologie, Inserm (Institut national de la santé et de la recherche médicale; UMR1071), INRAE (Institut national de recherche en agriculture, alimentation et environnement; USC 2018), the French government's Agence Nationale de la Recherche through the program "Investissements d'Avenir" (16-IDEX-0001 I-SITE CAP 20–25). **TM** was funded by a Carver Trust Collaborative Pilot Grant through the Carver College of Medicine at the University of Iowa. Support was provided in part by the American Cancer Society (Award Numbers ACS-IRG-15-176-41 and ACS-IRG-18-165-43) and by the Carver College of Medicine, University of Iowa Research Start-Up funds.

References

- [1] J. Hampe, A. Franke, P. Rosenstiel, A. Till, M. Teuber, K. Huse, M. Albrecht, G. Mayr, F.M. De La Vega, J. Briggs, S. Günther, N.J. Prescott, C.M. Onnie, R. Häsler, B. Sipos, U.R. Fölsch, T. Lengauer, M. Platzer, C.G. Mathew, M. Krawczak, S. Schreiber, A genome-wide

- association scan of nonsynonymous SNPs identifies a susceptibility variant for Crohn disease in ATG16L1, *Nat. Genet.* 39 (2006) 207–11. <https://doi.org/10.1038/ng1954>.
- [2] J.D. Rioux, R.J. Xavier, K.D. Taylor, M.S. Silverberg, P. Goyette, A. Huett, T. Green, P. Kuballa, M.M. Barmada, L.W. Datta, Y.Y. Shugart, A.M. Griffiths, S.R. Targan, A.F. Ippoliti, E.-J. Bernard, L. Mei, D.L. Nicolae, M. Regueiro, L.P. Schumm, A.H. Steinhart, J.I. Rotter, R.H. Duerr, J.H. Cho, M.J. Daly, S.R. Brant, Genome-wide association study identifies new susceptibility loci for Crohn disease and implicates autophagy in disease pathogenesis, *Nat. Genet.* 39 (2007) 596–604. <https://doi.org/10.1038/ng2032>.
- [3] M.F. Neurath, Targeting immune cell circuits and trafficking in inflammatory bowel disease, *Nat. Immunol.* 20 (2019) 970–979. <https://doi.org/10.1038/s41590-019-0415-0>.
- [4] Y. Zhen, H. Zhang, NLRP3 Inflammasome and Inflammatory Bowel Disease, *Front. Immunol.* 10 (2019) 276. <https://doi.org/10.3389/fimmu.2019.00276>.
- [5] A. Larabi, N. Barnich, H.T.T. Nguyen, New insights into the interplay between autophagy, gut microbiota and inflammatory responses in IBD, *Autophagy.* 16 (2020) 38–51. <https://doi.org/10.1080/15548627.2019.1635384>.
- [6] L. Huang, X. Mao, Y. Li, D. Liu, K. Fan, R. Liu, T. Wu, H. Wang, Y. Zhang, B. Yang, Multiomics analyses reveal a critical role of selenium in controlling T cell differentiation in Crohn’s disease, *Immunity.* 54 (2021) 1728–1744.e7. <https://doi.org/10.1016/j.immuni.2021.07.004>.
- [7] G.G. Kaplan, J.W. Windsor, The four epidemiological stages in the global evolution of inflammatory bowel disease, *Nat. Rev. Gastroenterol. Hepatol.* 18 (2021) 56–66. <https://doi.org/10.1038/s41575-020-00360-x>.
- [8] K.M. Hooper, P.G. Barlow, C. Stevens, P. Henderson, Inflammatory Bowel Disease Drugs: A Focus on Autophagy, *J. Crohn’s Colitis.* 11 (2017) 118–127. <https://doi.org/10.1093/ecco-jcc/jjw127>.
- [9] H. Herfarth, E.L. Barnes, J.F. Valentine, J. Hanson, P.D.R. Higgins, K.L. Isaacs, S. Jackson, M.T. Osterman, K. Anton, A. Ivanova, M.D. Long, C. Martin, R.S. Sandler, B. Abraham, R.K. Cross, G. Dryden, M. Fischer, W. Harlan, C. Levy, R. McCabe, S. Polyak, S. Saha, E. Williams, V. Yajnik, J. Serrano, B.E. Sands, J.D. Lewis, Methotrexate Is Not Superior to Placebo in Maintaining Steroid-Free Response or Remission in Ulcerative Colitis, *Gastroenterology.* 155 (2018) 1098–1108. <https://doi.org/10.1053/j.gastro.2018.06.046>.
- [10] S.V. Retnakumar, S. Muller, Pharmacological autophagy regulators as therapeutic agents for inflammatory bowel diseases, *Trends Mol. Med.* 25 (2019) 516–537. <https://doi.org/10.1016/j.molmed.2019.03.002>.
- [11] J.C. Martin, C. Chang, G. Boschetti, R. Ungaro, M. Giri, J.A. Grout, K. Gettler, L.-S. Chuang, S. Nayar, A.J. Greenstein, M. Dubinsky, L. Walker, A. Leader, J.S. Fine, C.E. Whitehurst, M.L. Mbow, S. Kugathasan, L.A. Denson, J.S. Hyams, J.R. Friedman, P.T. Desai, H.M. Ko, I. Laface, G. Akturk, E.E. Schadt, H. Salmon, S. Gnjatic, A.H. Rahman, M. Merad, J.H. Cho, E. Kenigsberg, Single-Cell Analysis of Crohn’s Disease Lesions Identifies a Pathogenic Cellular Module Associated with Resistance to Anti-TNF Therapy, *Cell.* 178 (2019) 1493–1508.e20. <https://doi.org/10.1016/j.cell.2019.08.008>.
- [12] M. Argollo, P.G. Kotze, P. Kakkadasam, G. D’Haens, Optimizing biologic therapy in IBD: how essential is therapeutic drug monitoring?, *Nat. Rev. Gastroenterol. Hepatol.* 17 (2020) 702–710. <https://doi.org/10.1038/s41575-020-0352-2>.
- [13] M. Friedrich, M. Pohin, M.A. Jackson, I. Korsunsky, S.J. Bullers, K. Rue-Albrecht, Z. Christoforidou, D. Sathananthan, T. Thomas, R. Ravindran, R. Tandon, R.S. Peres, H. Sharpe, K. Wei, G.F.M. Watts, E.H. Mann, A. Geremia, M. Attar, F. Barone, M. Brenner, C.D. Buckley, M. Coles, A.P. Frei, K.G. Lassen, F.M. Powrie, S. McCuaig, L. Thomas, E. Collantes, H.H. Uhlig, S.N. Sansom, A. Easton, S. Raychaudhuri, S.P. Travis, F.M. Powrie, O.I.B.D.C. Investigators, R.F.N. Consortium, IL-1-driven stromal–neutrophil interactions define a subset of patients with inflammatory bowel disease that does not respond to therapies, *Nat. Med.* 27 (2021) 1970–1981. <https://doi.org/10.1038/s41591-021-01520-5>.
- [14] W.J. Sandborn, R. Rebutck, Y. Wang, B. Zou, O.J. Adedokun, C. Gasink, B.E. Sands, S.B. Hanauer, S. Targan, S. Ghosh, W.J.S. de Villiers, J.-F. Colombel, B.G. Feagan, J.P. Lynch, Five-Year Efficacy and Safety of Ustekinumab Treatment in Crohn’s Disease: The IM-UNITI

- Trial, *Clin. Gastroenterol. Hepatol.* (2021). <https://doi.org/10.1016/j.cgh.2021.02.025>.
- [15] L. Goessens, J. Colombel, A. Outtier, M. Ferrante, J. Sabino, C. Judge, R. Saeidi, L. Rabbitt, A. Armuzzi, E. Domenech, Safety and efficacy of combining biologics or small molecules for inflammatory bowel disease or immune-mediated inflammatory diseases: A European retrospective observational study, *UEG J.* 9 (2021) 1136–1147. <https://doi.org/10.1002/ueg2.12170>.
- [16] B.G. Feagan, S. Danese, E. V Loftus Jr, S. Vermeire, S. Schreiber, T. Ritter, R. Fogel, R. Mehta, S. Nijhawan, R. Kempinski, Filgotinib as induction and maintenance therapy for ulcerative colitis (SELECTION): a phase 2b/3 double-blind, randomised, placebo-controlled trial, *Lancet.* 397 (2021) 2372–2384. [https://doi.org/10.1016/S0140-6736\(21\)00666-8](https://doi.org/10.1016/S0140-6736(21)00666-8).
- [17] P. Serra, P. Santamaria, Antigen-specific therapeutic approaches for autoimmunity, *Nat. Biotechnol.* 37 (2019) 238–251. <https://doi.org/10.1038/s41587-019-0015-4>.
- [18] R.N. Kostoff, M.B. Briggs, D.R. Shores, Treatment repurposing for inflammatory bowel disease using literature-related discovery and innovation, *World J. Gastroenterol.* 26 (2020) 4889–4899. <https://doi.org/10.3748/wjg.v26.i33.4889>.
- [19] F. Monneaux, J.M. Lozano, M.E. Patarroyo, J. Briand, S. Muller, T cell recognition and therapeutic effect of a phosphorylated synthetic peptide of the 70K snRNP protein administered in MRL/lpr mice, *Eur. J. Immunol.* 33 (2003) 287–296. <https://doi.org/10.1002/immu.200310002>.
- [20] F. Wang, I. Tasset, A.M. Cuervo, S. Muller, In Vivo Remodeling of Altered Autophagy-Lysosomal Pathway by a Phosphopeptide in Lupus, *Cells.* 9 (2020) 2328. <https://doi.org/10.3390/cells9102328>.
- [21] N. Page, F. Gros, N. Schall, M. Décossas, D. Bagnard, J.-P. Briand, S. Muller, HSC70 blockade by the therapeutic peptide P140 affects autophagic processes and endogenous MHCII presentation in murine lupus, *Ann. Rheum. Dis.* 70 (2011) 837–843. <https://doi.org/10.1136/ard.2010.139832>.
- [22] C. Macri, F. Wang, I. Tasset, N. Schall, N. Page, J.-P. Briand, A.M. Cuervo, S. Muller, Modulation of deregulated chaperone-mediated autophagy by a phosphopeptide, *Autophagy.* 11 (2015) 472–486. <https://doi.org/10.1080/15548627.2015.1017179>.
- [23] B. Li, F. Wang, N. Schall, S. Muller, Rescue of autophagy and lysosome defects in salivary glands of MRL/lpr mice by a therapeutic phosphopeptide, *J. Autoimmun.* 90 (2018) 132–145. <https://doi.org/10.1016/j.jaut.2018.02.005>.
- [24] E. Voynova, F. Lefebvre, A. Qadri, S. Muller, Correction of autophagy impairment inhibits pathology in the NOD. H-2h4 mouse model of primary Sjögren’s syndrome, *J. Autoimmun.* 108 (2020) 102418. <https://doi.org/10.1016/j.jaut.2020.102418>.
- [25] S. Brun, N. Schall, S.R. Bonam, K. Bigaut, A.-G. Mensah-Nyagan, J. de Sèze, S. Muller, An autophagy-targeting peptide to treat chronic inflammatory demyelinating polyneuropathies, *J. Autoimmun.* 92 (2018) 114–125. <https://doi.org/10.1016/j.jaut.2018.05.009>.
- [26] F. Daubeuf, N. Schall, N. Petit-Demoulière, N. Frossard, S. Muller, An Autophagy Modulator Peptide Prevents Lung Function Decrease and Corrects Established Inflammation in Murine Models of Airway Allergy, *Cells.* 10 (2021) 2468. <https://doi.org/10.3390/cells10092468>.
- [27] Y. Momozawa, J. Dmitrieva, E. Théâtre, V. Deffontaine, S. Rahmouni, B. Charlotteaux, F. Crins, E. Docampo, M. Elansary, A.-S. Gori, C. Lecut, R. Mariman, M. Mni, C. Oury, I. Altukhov, D. Alexeev, Y. Aulchenko, L. Amininejad, G. Bouma, F. Hoentjen, M. Löwenberg, B. Oldenburg, M.J. Pierik, A.E. vander Meulen-de Jong, C. Janneke van der Woude, M.C. Visschedijk, C. Abraham, J.-P. Achkar, T. Ahmad, A.N. Ananthakrishnan, V. Andersen, C.A. Anderson, J.M. Andrews, V. Anese, G. Aumais, L. Baidoo, R.N. Baldassano, P.A. Bampton, M. Barclay, J.C. Barrett, T.M. Bayless, J. Bethge, A. Bitton, G. Boucher, S. Brand, B. Brandt, S.R. Brant, C. Büning, A. Chew, J.H. Cho, I. Cleylen, A. Cohain, A. Croft, M.J. Daly, M. D’Amato, S. Danese, D. De Jong, G. Denapiene, L.A. Denson, K.L. Devaney, O. Dewit, R. D’Inca, M. Dubinsky, R.H. Duerr, C. Edwards, D. Ellinghaus, J. Essers, L.R. Ferguson, E.A. Festen, P. Fleshner, T. Florin, A. Franke, K. Fransen, R. Gearry, C. Gieger, J. Glas, P. Goyette, T. Green, A.M. Griffiths, S.L. Guthery, H. Hakonarson, J. Halfvarson, K. Hanigan, T. Haritunians, A. Hart, C. Hawkey, N.K. Hayward, M. Hedl, P. Henderson, X. Hu, H. Huang, K.Y. Hui, M. Imielinski, A. Ippoliti, L. Jonaitis, L. Jostins, T.H. Karlsen, N.A. Kennedy, M.A.

- Khan, G. Kiudelis, K. Krishnaprasad, S. Kugathasan, L. Kupcinskas, A. Latiano, D. Laukens, I.C. Lawrance, J.C. Lee, C.W. Lees, M. Leja, J. Van Limbergen, P. Lionetti, J.Z. Liu, G. Mahy, J. Mansfield, D. Massey, C.G. Mathew, D.P.B. McGovern, R. Milgrom, M. Mitrovic, G.W. Montgomery, C. Mowat, W. Newman, A. Ng, S.C. Ng, S.M.E. Ng, S. Nikolaus, K. Ning, M. Nöthen, I. Oikonomou, O. Palmieri, M. Parkes, A. Phillips, C.Y. Ponsioen, U. Potocnik, N.J. Prescott, D.D. Proctor, G. Radford-Smith, J.-F. Rahier, S. Raychaudhuri, M. Regueiro, F. Rieder, J.D. Rioux, S. Ripke, R. Roberts, R.K. Russell, J.D. Sanderson, M. Sans, J. Satsangi, E.E. Schadt, S. Schreiber, D. Schulte, L.P. Schumm, R. Scott, M. Seielstad, Y. Sharma, M.S. Silverberg, L.A. Simms, J. Skieceviciene, S.L. Spain, A.H. Steinhart, J.M. Stempak, L. Stronati, J. Sventoraityte, S.R. Targan, K.M. Taylor, A. ter Velde, L. Torkvist, M. Tremelling, S. van Sommeren, E. Vasiliauskas, H.W. Verspaget, T. Walters, K. Wang, M.-H. Wang, Z. Wei, D. Whiteman, C. Wijmenga, D.C. Wilson, J. Winkelmann, R.J. Xavier, B. Zhang, C.K. Zhang, H. Zhang, W. Zhang, H. Zhao, Z.Z. Zhao, M. Lathrop, J.-P. Hugot, R.K. Weersma, M. De Vos, D. Franchimont, S. Vermeire, M. Kubo, E. Louis, M. Georges, T.I.I.B.D.G. Consortium, IBD risk loci are enriched in multigenic regulatory modules encompassing putative causative genes, *Nat. Commun.* 9 (2018) 2427. <https://doi.org/10.1038/s41467-018-04365-8>.
- [28] M. Friedrich, M. Pohin, F. Powrie, Cytokine Networks in the Pathophysiology of Inflammatory Bowel Disease, *Immunity*. 50 (2019) 992–1006. <https://doi.org/10.1016/j.immuni.2019.03.017>.
- [29] B. Huang, Z. Chen, L. Geng, J. Wang, H. Liang, Y. Cao, H. Chen, W. Huang, M. Su, H. Wang, Y. Xu, Y. Liu, B. Lu, H. Xian, H. Li, H. Li, L. Ren, J. Xie, L. Ye, H. Wang, J. Zhao, P. Chen, L. Zhang, S. Zhao, T. Zhang, B. Xu, D. Che, W. Si, X. Gu, L. Zeng, Y. Wang, D. Li, Y. Zhan, D. Delfouneso, A.M. Lew, J. Cui, W.H. Tang, Y. Zhang, S. Gong, F. Bai, M. Yang, Y. Zhang, Mucosal Profiling of Pediatric-Onset Colitis and IBD Reveals Common Pathogenics and Therapeutic Pathways, *Cell*. 179 (2019) 1160-1176.e24. <https://doi.org/10.1016/j.cell.2019.10.027>.
- [30] C.S. Smillie, M. Biton, J. Ordovas-Montanes, K.M. Sullivan, G. Burgin, D.B. Graham, R.H. Herbst, N. Rogel, M. Slyper, J. Waldman, M. Sud, E. Andrews, G. Velonias, A.L. Haber, K. Jagadeesh, S. Vickovic, J. Yao, C. Stevens, D. Dionne, L.T. Nguyen, A.-C. Villani, M. Hofree, E.A. Creasey, H. Huang, O. Rozenblatt-Rosen, J.J. Garber, H. Khalili, A.N. Desch, M.J. Daly, A.N. Ananthakrishnan, A.K. Shalek, R.J. Xavier, A. Regev, Intra- and Inter-cellular Rewiring of the Human Colon during Ulcerative Colitis, *Cell*. 178 (2019) 714-730.e22. <https://doi.org/10.1016/j.cell.2019.06.029>.
- [31] L. Henckaerts, I. Cleynen, M. Brinar, J.M. John, K. Van Steen, P. Rutgeerts, S. Vermeire, Genetic variation in the autophagy gene ULK1 and risk of Crohn’s disease, *Inflamm. Bowel Dis.* 17 (2011) 1392–1397. <https://doi.org/10.1002/ibd.21486>.
- [32] J. Glas, J. Seiderer, S. Bues, J. Stallhofer, C. Fries, T. Olszak, E. Tsekere, M. Wetzke, F. Beigel, C. Steib, M. Friedrich, B. Göke, J. Diegelmann, D. Czamara, S. Brand, IRGM variants and susceptibility to inflammatory bowel disease in the german population, *PLoS One*. 8 (2013) e54338. <https://doi.org/10.1371/journal.pone.0054338>.
- [33] X.C. Lu, Y. Tao, C. Wu, P.L. Zhao, K. Li, J.Y. Zheng, L.X. Li, Association between variants of the autophagy related gene – IRGM and susceptibility to Crohn’s disease and ulcerative colitis: a meta-analysis, *PLoS One*. 8 (2013) e80602. <https://doi.org/10.1371/journal.pone.0080602>.
- [34] T. Iida, Y. Yokoyama, K. Wagatsuma, D. Hirayama, H. Nakase, Impact of Autophagy of Innate Immune Cells on Inflammatory Bowel Disease, *Cells*. 8 (2018) 7. <https://doi.org/10.3390/cells8010007>.
- [35] S. Kim, H.S. Eun, E.-K. Jo, Roles of Autophagy-Related Genes in the Pathogenesis of Inflammatory Bowel Disease, *Cells*. 8 (2019) 77. <https://doi.org/10.3390/cells8010077>.
- [36] C. Ma, C.E. Storer, U. Chandran, W.A. LaFramboise, P. Petrosko, M. Frank, D.J. Hartman, L. Pantanowitz, T. Haritunians, R.D. Head, T.-C. Liu, Crohn’s disease-associated ATG16L1 T300A genotype is associated with improved survival in gastric cancer, *EBioMedicine*. 67 (2021) 103347. <https://doi.org/10.1016/j.ebiom.2021.103347>.
- [37] C. Strisciuglio, E. Miele, M.E. Wildenberg, F.P. Giugliano, M. Andrezzi, A. Vitale, F. Capasso, A. Camarca, M. V Barone, A. Staiano, T300A variant of autophagy ATG16L1 gene

- is associated with decreased antigen sampling and processing by dendritic cells in pediatric Crohn's disease, *Inflamm. Bowel Dis.* 19 (2013) 2339–2348. <https://doi.org/10.1097/MIB.0b013e3182a6a11c>.
- [38] J. Pott, K.J. Maloy, Epithelial autophagy controls chronic colitis by reducing TNF-induced apoptosis, *Autophagy*. (2018). <https://doi.org/10.1080/15548627.2018.1450021>.
- [39] J. Pott, A.M. Kabat, K.J. Maloy, Intestinal Epithelial Cell Autophagy Is Required to Protect against TNF-Induced Apoptosis during Chronic Colitis in Mice., *Cell Host Microbe*. 23 (2018) 191–202. <https://doi.org/10.1016/j.chom.2017.12.017>.
- [40] P.K. Nighot, C.-A.A. Hu, T.Y. Ma, Autophagy enhances intestinal epithelial tight junction barrier function by targeting claudin-2 protein degradation., *J. Biol. Chem.* 290 (2015) 7234–7246. <https://doi.org/10.1074/jbc.M114.597492>.
- [41] B. Shai, P. Mihir, W. Yuhao, L. Yun, R.K. A., H. Brian, L. Tess, W.S. E., X.R. J., H.L. V., Paneth cells secrete lysozyme via secretory autophagy during bacterial infection of the intestine, *Science*. 357 (2017) 1047–1052. <https://doi.org/10.1126/science.aal4677>.
- [42] K.K. Patel, H. Miyoshi, W.L. Beatty, R.D. Head, N.P. Malvin, K. Cadwell, J.-L. Guan, T. Saitoh, S. Akira, P.O. Seglen, M.C. Dinauer, H.W. Virgin, T.S. Stappenbeck, Autophagy proteins control goblet cell function by potentiating reactive oxygen species production, *EMBO J.* 32 (2013) 3130–3144. <https://doi.org/10.1038/emboj.2013.233>.
- [43] T. Saitoh, N. Fujita, M.H. Jang, S. Uematsu, B.-G. Yang, T. Satoh, H. Omori, T. Noda, N. Yamamoto, M. Komatsu, K. Tanaka, T. Kawai, T. Tsujimura, O. Takeuchi, T. Yoshimori, S. Akira, Loss of the autophagy protein Atg16L1 enhances endotoxin-induced IL-1 β production, *Nature*. 456 (2008) 264–8. <https://doi.org/10.1038/nature07383>.
- [44] R. Cooney, J. Baker, O. Brain, B. Danis, T. Pichulik, P. Allan, D.J.P. Ferguson, B.J. Campbell, D. Jewell, A. Simmons, NOD2 stimulation induces autophagy in dendritic cells influencing bacterial handling and antigen presentation, *Nat. Med.* 16 (2010) 90–97. <https://doi.org/10.1038/nm.2069>.
- [45] K. Tsuboi, M. Nishitani, A. Takakura, Y. Imai, M. Komatsu, H. Kawashima, Autophagy Protects against Colitis by the Maintenance of Normal Gut Microflora and Secretion of Mucus., *J. Biol. Chem.* 290 (2015) 20511–20526. <https://doi.org/10.1074/jbc.M114.632257>.
- [46] S. Lavoie, K.L. Conway, K.G. Lassen, H.B. Jijon, H. Pan, E. Chun, M. Michaud, J.K. Lang, C.A.G. Comeau, J.M. Dreyfuss, The Crohn's disease polymorphism, ATG16L1 T300A, alters the gut microbiota and enhances the local Th1/Th17 response, *Elife*. 8 (2019) e39982. <https://doi.org/10.7554/eLife.39982.001>.
- [47] R. Geesala, W. Schanz, M. Biggs, G. Dixit, J. Skurski, P. Gurung, D.K. Meyerholz, D. Elliott, P.D. Issuree, T. Maretzky, Loss of RHBDF2 results in an early-onset spontaneous murine colitis, *J. Leukoc. Biol.* 105 (2019) 767–781. <https://doi.org/10.1002/JLB.4A0718-283RR>.
- [48] N. Page, N. Schall, J.-M. Strub, M. Quinternet, O. Chaloin, M. Décossas, M.T. Cung, A. Van Dorsselaer, J.-P. Briand, S. Muller, The spliceosomal phosphopeptide P140 controls the lupus disease by interacting with the HSC70 protein and via a mechanism mediated by $\gamma\delta$ T cells, *PLoS One*. 4 (2009) e5273. <https://doi.org/10.1371/journal.pone.0005273>.
- [49] K. Suzuki, X. Sun, M. Nagata, T. Kawase, H. Yamaguchi, V. Sukumaran, Y. Kawachi, H. Kawachi, T. Nishino, K. Watanabe, H. Yoneyama, H. Asakura, Analysis of intestinal fibrosis in chronic colitis in mice induced by dextran sulfate sodium, *Pathol. Int.* 61 (2011) 228–238. <https://doi.org/10.1111/j.1440-1827.2011.02647.x>.
- [50] H. Sann, J. von Erichsen, M. Hessmann, A. Pahl, A. Hoffmeyer, Efficacy of drugs used in the treatment of IBD and combinations thereof in acute DSS-induced colitis in mice, *Life Sci.* 92 (2013) 708–718. <https://doi.org/10.1016/j.lfs.2013.01.028>.
- [51] P. Desreumaux, L. Dubuquoy, S. Nutten, M. Peuchmaur, W. Englaro, K. Schoonjans, B. Derijard, B. Desvergne, W. Wahli, P. Chambon, M.D. Leibowitz, J.F. Colombel, J. Auwerx, Attenuation of colon inflammation through activators of the retinoid X receptor (RXR)/peroxisome proliferator-activated receptor γ (PPAR γ) heterodimer: A basis for new therapeutic strategies, *J. Exp. Med.* 193 (2001) 827–838. <https://doi.org/10.1084/jem.193.7.827>.
- [52] F. Wang, B. Li, N. Schall, M. Wilhelm, S. Muller, Assessing Autophagy in Mouse Models and Patients with Systemic Autoimmune Diseases, *Cells*. 6 (2017) 16.

- <https://doi.org/10.3390/cells6030016>.
- [53] B. Siegmund, H.-A. Lehr, G. Fantuzzi, C.A. Dinarello, IL-1 β -converting enzyme (caspase-1) in intestinal inflammation, *Proc. Natl. Acad. Sci.* 98 (2001) 13249–13254. <https://doi.org/10.1073/pnas.231473998>.
- [54] T. Vowinkel, T.J. Kalogeris, M. Mori, C.F. Krieglstein, D.N. Granger, Impact of dextran sulfate sodium load on the severity of inflammation in experimental colitis, *Dig. Dis. Sci.* 49 (2004) 556–564. <https://doi.org/10.1023/B:DDAS.0000026298.72088.f7>.
- [55] S. Wirtz, V. Popp, M. Kindermann, K. Gerlach, B. Weigmann, S. Fichtner-Feigl, M.F. Neurath, Chemically induced mouse models of acute and chronic intestinal inflammation, *Nat. Protoc.* 12 (2017) 1295–1309. <https://doi.org/10.1038/nprot.2017.044>.
- [56] M. Perše, A. Cerar, Dextran sodium sulphate colitis mouse model: traps and tricks, *Biomed Res. Int.* 2012 (2012) 718617. <https://doi.org/10.1155/2012/718617>.
- [57] I. Silva, R. Pinto, V. Mateus, Preclinical Study in Vivo for New Pharmacological Approaches in Inflammatory Bowel Disease: A Systematic Review of Chronic Model of TNBS-Induced Colitis, *J. Clin. Med.* 8 (2019) 1574. <https://doi.org/10.3390/jcm8101574>.
- [58] E. Antoniou, G.A. Margonis, A. Angelou, A. Pikouli, P. Argiri, I. Karavokyros, A. Papalois, E. Pikoulis, The TNBS-induced colitis animal model: An overview, *Ann. Med. Surg.* 11 (2016) 9–15. <https://doi.org/10.1016/j.amsu.2016.07.019>.
- [59] A. Bleich, M. Mähler, C. Most, E.H. Leiter, E. Liebler–Tenorio, C.O. Elson, H.J. Hedrich, B. Schlegelberger, J.P. Sundberg, Refined histopathologic scoring system improves power to detect colitis QTL in mice, *Mamm. Genome.* 15 (2004) 865–871. <https://doi.org/10.1007/s00335-004-2392-2>.
- [60] L.A. Dieleman, M.J. Palmen, H. Akol, E. Bloemena, A.S. Peña, S.G. Meuwissen, E.P. Van Rees, Chronic experimental colitis induced by dextran sulphate sodium (DSS) is characterized by Th1 and Th2 cytokines, *Clin. Exp. Immunol.* 114 (1998) 385–391. <https://doi.org/10.1046/j.1365-2249.1998.00728.x>.
- [61] P. Alex, N.C. Zachos, T. Nguyen, L. Gonzales, T.-E. Chen, L.S. Conklin, M. Centola, X. Li, Distinct cytokine patterns identified from multiplex profiles of murine DSS and TNBS-induced colitis, *Inflamm. Bowel Dis.* 15 (2009) 341–352. <https://doi.org/10.1002/ibd.20753>.
- [62] P. Kiesler, I.J. Fuss, W. Strober, Experimental models of inflammatory bowel diseases, *Cell. Mol. Gastroenterol. Hepatol.* 1 (2015) 154–170. [https://doi.org/10.1016/0016-5085\(95\)90599-5](https://doi.org/10.1016/0016-5085(95)90599-5).
- [63] B.-Z. Shao, Y. Yao, J.-S. Zhai, J.-H. Zhu, J.-P. Li, K. Wu, The role of autophagy in inflammatory bowel disease, *Front. Physiol.* 12 (2021). <https://doi.org/10.3389/fphys.2021.621132>.
- [64] D.J. Klionsky, A.K. Abdel-Aziz, S. Abdelfatah, M. Abdellatif, A. Abdoli, S. Abel, H. Abeliovich, M.H. Abildgaard, Y.P. Abudu, A. Acevedo-Arozena, Guidelines for the use and interpretation of assays for monitoring autophagy, *Autophagy.* 17 (2021) 1–382. <https://doi.org/10.1080/15548627.2015.1100356>.
- [65] P. Jiang, N. Mizushima, LC3- and p62-based biochemical methods for the analysis of autophagy progression in mammalian cells, *Methods.* 75 (2015) 13–18. <https://doi.org/10.1016/j.ymeth.2014.11.021>.
- [66] J. Peng, S. Han, Z. Chen, J. Yang, Y. Pei, C. Bao, L. Qiao, W. Chen, B. Liu, Chaperone-mediated autophagy regulates apoptosis and the proliferation of colon carcinoma cells, *Biochem. Biophys. Res. Commun.* 522 (2020) 348–354. <https://doi.org/10.1016/j.bbrc.2019.11.081>.
- [67] S. Kaushik, U. Bandyopadhyay, S. Sridhar, R. Kiffin, M. Martinez-Vicente, M. Kon, S.J. Orenstein, E. Wong, A.M. Cuervo, Chaperone-mediated autophagy at a glance, *J. Cell Sci.* 124 (2011) 495–499. <https://doi.org/10.1242/jcs.073874>.
- [68] F. Hu, G. Li, C. Huang, Z. Hou, X. Yang, X. Luo, Y. Feng, G. Wang, J. Hu, Z. Cao, The autophagy-independent role of BECN1 in colorectal cancer metastasis through regulating STAT3 signaling pathway activation, *Cell Death Dis.* 11 (2020) 304. <https://doi.org/10.1038/s41419-020-2467-3>.
- [69] S.B. Thoresen, N.M. Pedersen, K. Liestøl, H. Stenmark, A phosphatidylinositol 3-kinase class III sub-complex containing VPS15, VPS34, Beclin 1, UVRAG and BIF-1 regulates cytokinesis

- and degradative endocytic traffic, *Exp. Cell Res.* 316 (2010) 3368–3378. <https://doi.org/10.1016/j.yexcr.2010.07.008>.
- [70] J. Diao, R. Liu, Y. Rong, M. Zhao, J. Zhang, Y. Lai, Q. Zhou, L.M. Wilz, J. Li, S. Vivona, ATG14 promotes membrane tethering and fusion of autophagosomes to endolysosomes, *Nature*. 520 (2015) 563–566. <https://doi.org/10.1038/nature14147>.
- [71] G. Fiorino, G.C. Sturniolo, F. Bossa, A. Cassinotti, A. di Sabatino, P. Giuffrida, S. Danese, A Phase 2a, Multicenter, Randomized, Double-Blind, Parallel-Group, Placebo-Controlled Trial of IBD98-M Delayed-Release Capsules to Induce Remission in Patients with Active and Mild to Moderate Ulcerative Colitis, *Cells*. 8 (2019) 523. <https://doi.org/10.3390/cells8060523>.
- [72] B. Owens, Poor phase 4 safety results for tofacitinib raise questions about JAK inhibitors, *Lancet Rheumatol.* 3 (2021) e252. [https://doi.org/10.1016/S2665-9913\(21\)00071-0](https://doi.org/10.1016/S2665-9913(21)00071-0).
- [73] H. Shen, S. Zhang, W. Zhao, S. Ren, X. Ke, Q. Gu, Z. Tang, J. Xie, S. Chen, Y. Chen, J. Zou, L. Zhang, Z. Shen, K. Zheng, Y. Liu, P. Gu, J. Cheng, J. Hu, L. Zhu, Randomised clinical trial: Efficacy and safety of Qing-Chang-Hua-Shi granules in a multicenter, randomized, and double-blind clinical trial of patients with moderately active ulcerative colitis, *Biomed. Pharmacother.* 139 (2021) 111580. <https://doi.org/10.1016/j.biopha.2021.111580>.
- [74] R. Zimmer, H.R. Scherbarth, O.L. Rillo, J.J. Gomez-Reino, S. Muller, Lupuzor/P140 peptide in patients with systemic lupus erythematosus: a randomised, double-blind, placebo-controlled phase IIb clinical trial, *Ann. Rheum. Dis.* 72 (2013) 1830–1835. <https://doi.org/10.1136/annrheumdis-2012-202460>.
- [75] N. Schall, S. Muller, Resetting the autoreactive immune system with a therapeutic peptide in lupus, *Lupus*. 24 (2015) 412–418. <https://doi.org/10.1177/0961203314556138>.
- [76] T. Kökten, S. Gibot, P. Lepage, S. D’Alessio, J. Hablot, N.-C. Ndiaye, H. Busby-Venner, C. Monot, B. Garnier, D. Moulin, TREM-1 inhibition restores impaired autophagy activity and reduces colitis in mice, *J. Crohn Colitis*. 12 (2018) 230–244. <https://doi.org/10.1093/ecco-jcc/jjx129>.
- [77] G. Privitera, D. Pugliese, S. Onali, V. Petito, F. Scaldaferrri, A. Gasbarrini, S. Danese, A. Armuzzi, Combination therapy in inflammatory bowel disease—from traditional immunosuppressors towards the new paradigm of dual targeted therapy, *Autoimmun. Rev.* (2021) 102832. <https://doi.org/10.1016/j.autrev.2021.102832>.

Legends to Figures

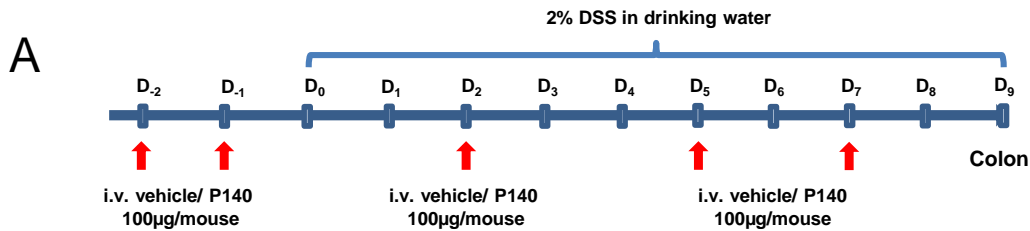
Figure 1. Experimental protocols. Schematic representation of experimental protocols and treatment regimens applied with the DSS-induced (Exp. A, B and C) and TNBS (Exp. D and E) mouse models of colitis. A-E show Exp. A to E, as referenced in the text. ScP140 was not used in Exp. A. Vehicle was NaCl 0.9% w/v. % DSS is expressed as w/v. EtOH, ethanol.

Figure 2. Therapeutic effects of P140 on DSS-induced colitis. Animals were treated with P140, ScP140, or vehicle alone (Exp. A, B, C). The clinical parameters shown in the figure are DAI (A, D, G), colon length (B, E, H; post-mortem measurement) and the presence of blood in stools (C, F, I). In Exp. A histopathological score could not be defined. Histology is shown for Exp. B (supplementary figure 2). Data are mean \pm SEM. *P* values were calculated using a Mann-Whitney U test (A, B, C), one-way (E), or two-way ANOVA (D, F, G, I) followed by Holm-Sidak's multiple comparisons; or a Kruskal-Wallis test followed by Dunn's multiple comparisons (E). Vehicle, NaCl 0.9% w/v; ns, non-significant.

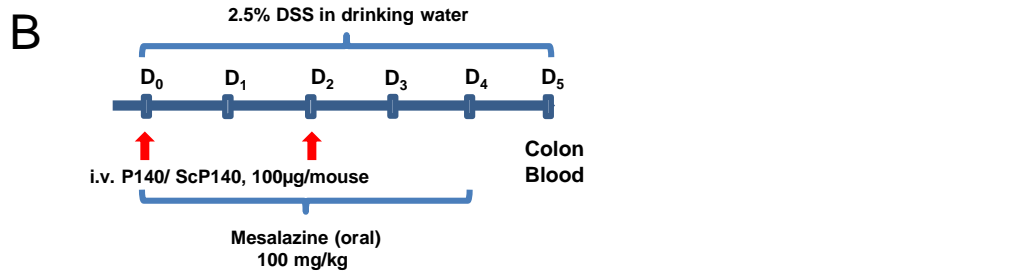
Figure 3. Therapeutic effects of P140 on TNBS-induced colitis. Animals were treated with P140, ScP140, or vehicle alone (Exp. E). A. body-weight percentage; B. Percent mortality; C. Wallace's score; D. Representative images of H&E staining. Black arrows indicate inflammatory cell infiltration and arrowheads indicate disrupted epithelium; scale bars 100 μ m. E. Ameho score; F. MPO activity. G. Representative western blot images for MAP1LC3B and SQSTM1 in spleen tissue. H. Quantification of protein expression levels normalized relative to total protein. Data are shown as mean \pm SEM. *P* values were calculated using a one-way (F) or 2-way ANOVA (A) followed by Holm-Sidak's multiple comparisons, a permutation test for two independent samples (C, E), or a Kruskal-Wallis test followed by Dunn's multiple comparisons (H). Vehicle, NaCl 0.9% w/v; ns, non-significant. EtOH, ethanol.

Figure 4. Therapeutic effects of P140 treatment in *il10^{-/-}iRhom2^{-/-}* mice. Mice were **let untreated** or treated with either P140 or ScP140 for 11 weeks (twice per week); A. Experimental design; B. Survival (n = 4-8 per group); C. Body-weight measured over the course of treatment; D. Representative photomicrographs of colons from **untreated** and P140- and ScP140-treated *il10^{-/-}iRhom2^{-/-}* mice; E. Colon length. F. Spleen weight and representative images of spleens from P140 and ScP140-treated *il10^{-/-}iRhom2^{-/-}* mice. *P* values were calculated using **log-rank (Mantel-Cox) test (B), Mann-whitney test (C) and two tailed unpaired Student's t test (E,F).**

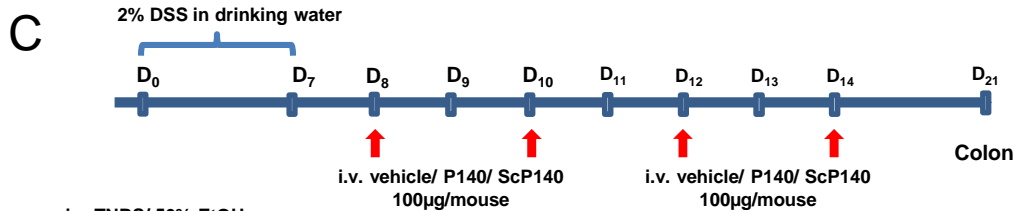
Figure 5. Effect of P140 on pro-inflammatory mediator production and selected autophagy markers in the colon from DSS-treated mice. Data are from Exp. A. A-E. mRNA expression levels for *Tnfa*, *Il6*, *Kc/Cxcl1*, *Mcp1/Ccl2* and *Il12* measured by qPCR. Results were normalized relative to levels of housekeeping reference *36b4* or *Pgk1*, *Actb* and *Ywhaz*; n = 7-9 per group. Data are mean \pm SEM. Statistical analysis: Mann-Whitney U test. F-J. Western blots and quantification of autophagy markers present in uninduced colon cells, or following DSS-induction and treatment with either vehicle or P140. F. Results from three representative mice. Signals were normalized relative to total protein content measured directly on the membrane (stain-free procedure). K,L. Representative immunofluorescence images, and quantification of SQSTM1 expression. Scale bars 50 μ m. Results are expressed as mean \pm SEM; Statistical analysis: one-way ANOVA followed by Holm-Sidak's multiple comparisons. Vehicle, NaCl 0.9% w/v; ns, non-significant.



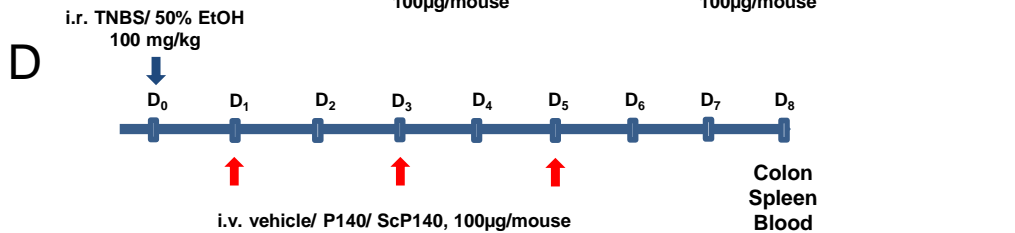
Group No.	No. of mice	Inducer	Therapy
1	9	DSS	Vehicle
2	9	DSS	P140



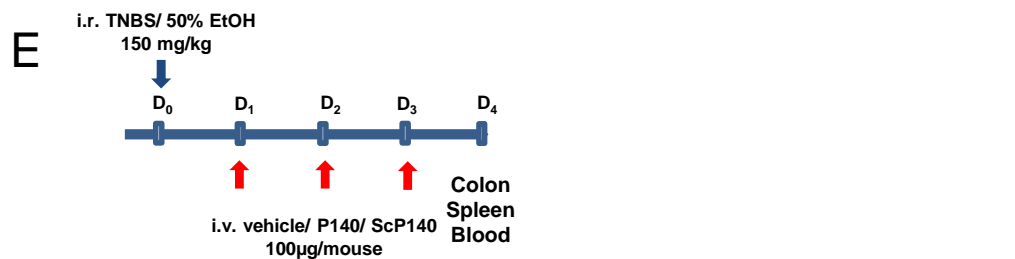
Group No.	No. of mice	Inducer	Therapy
1	8	DSS	P140
2	8	DSS	ScP140
3	8	DSS	Mesalazine



Group No.	No. of mice	Inducer	Therapy
1	10	DSS	Vehicle
2	10	DSS	P140
3	10	DSS	ScP140



Group No.	No. of mice	Inducer	Therapy
1	20	Ethanol	Vehicle
2	20	TNBS	Vehicle
3	20	TNBS	P140
4	10	TNBS	ScP140



Group No.	No. of mice	Inducer	Therapy
1	5	Ethanol	Vehicle
2	20	TNBS	Vehicle
3	20	TNBS	P140
4	20	TNBS	ScP140

Figure 1

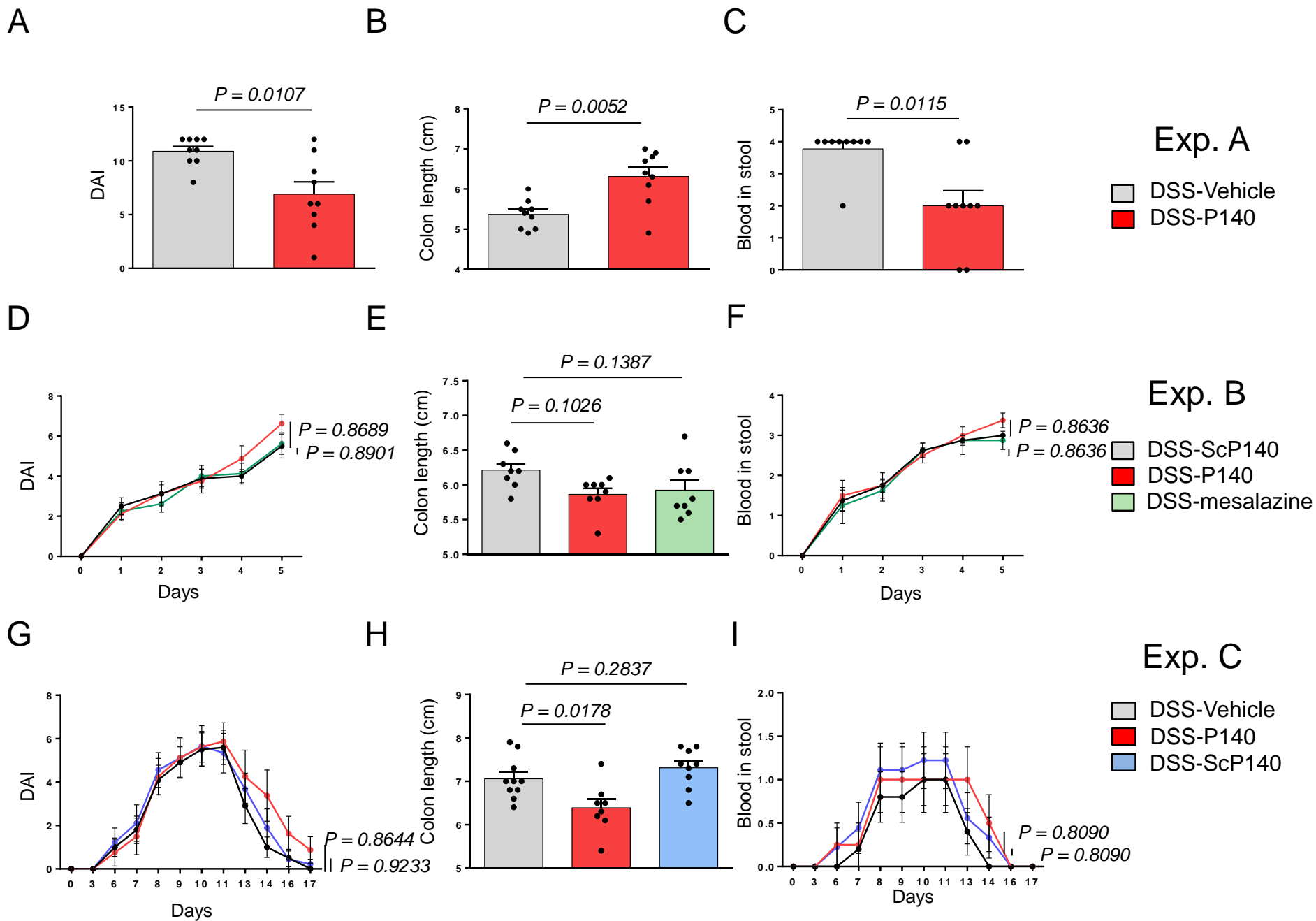
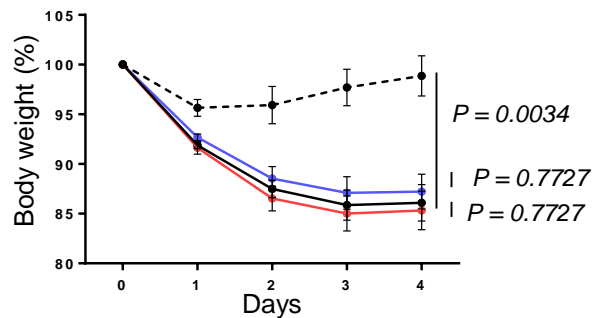
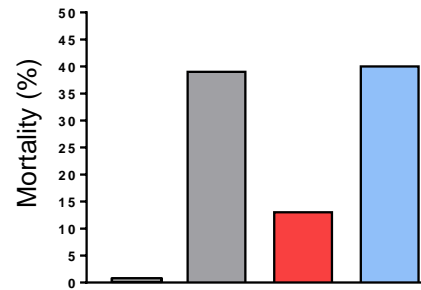


Figure 2

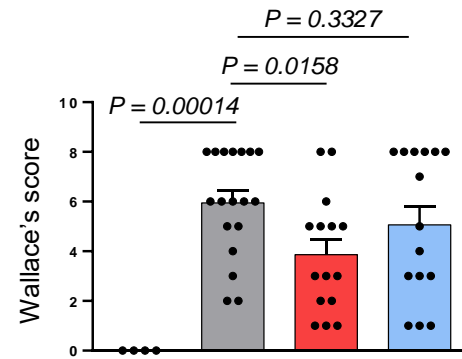
A



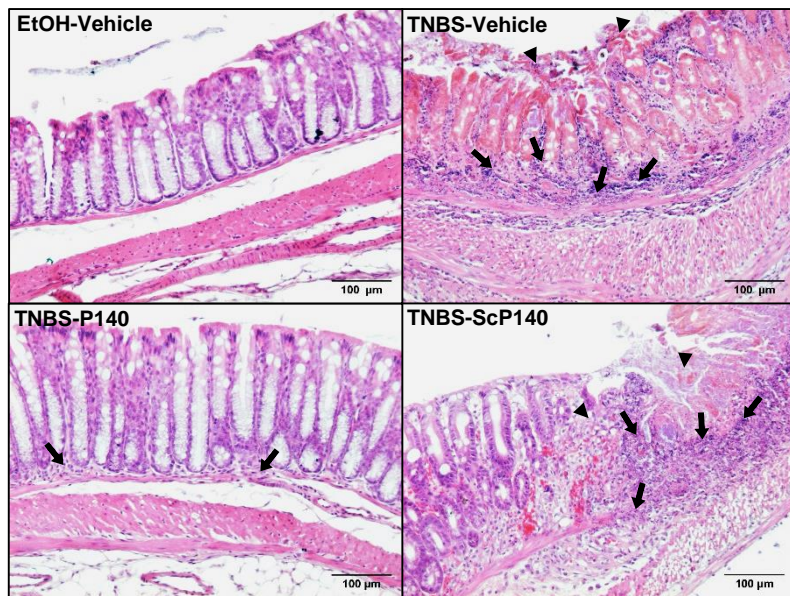
B



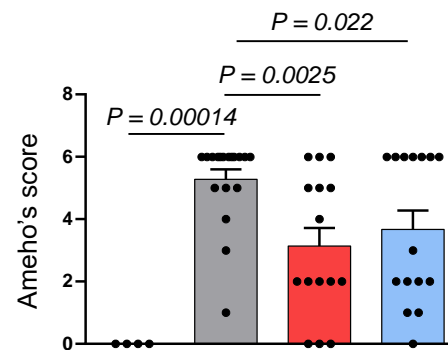
C



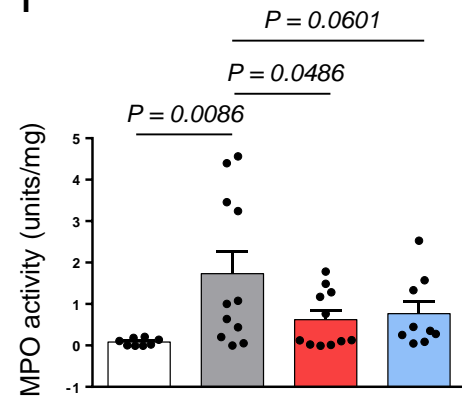
D



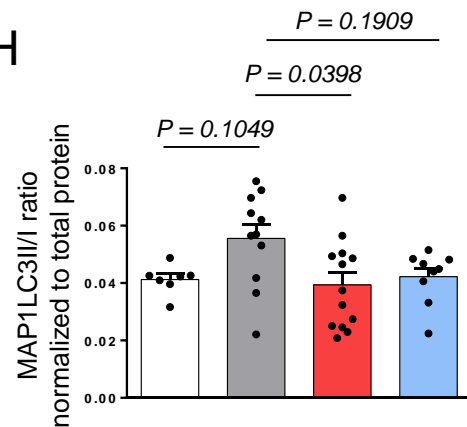
E



F



H



□ Ethanol-Vehicle
 ■ TNBS-Vehicle
 ■ TNBS-P140
 ■ TNBS-ScP140

G

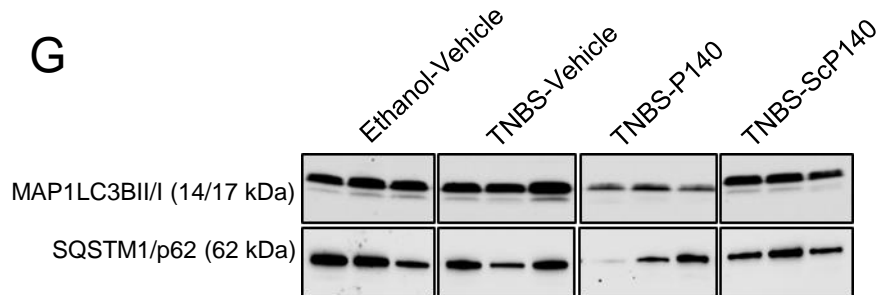


Figure 3

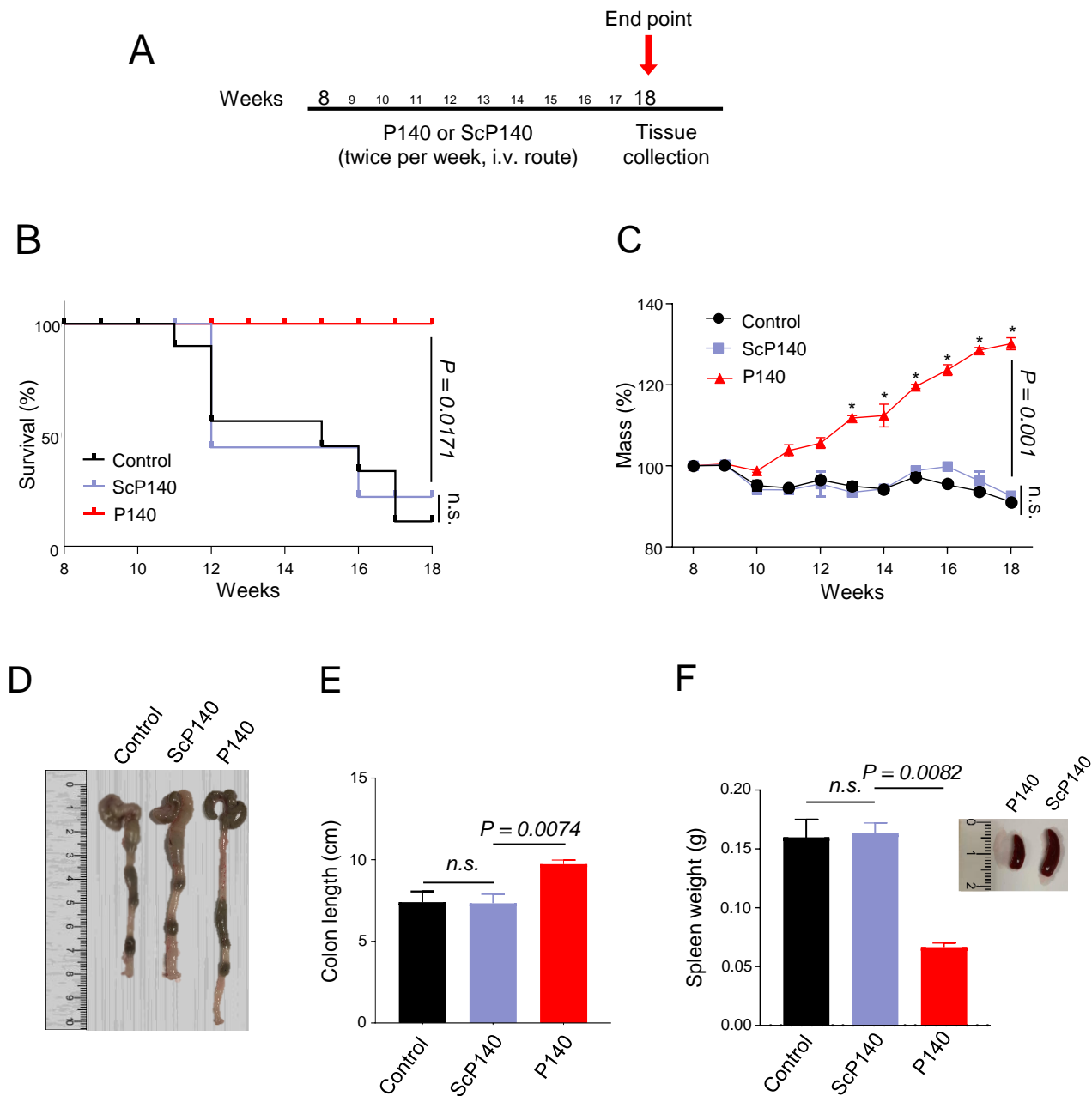


Figure 4

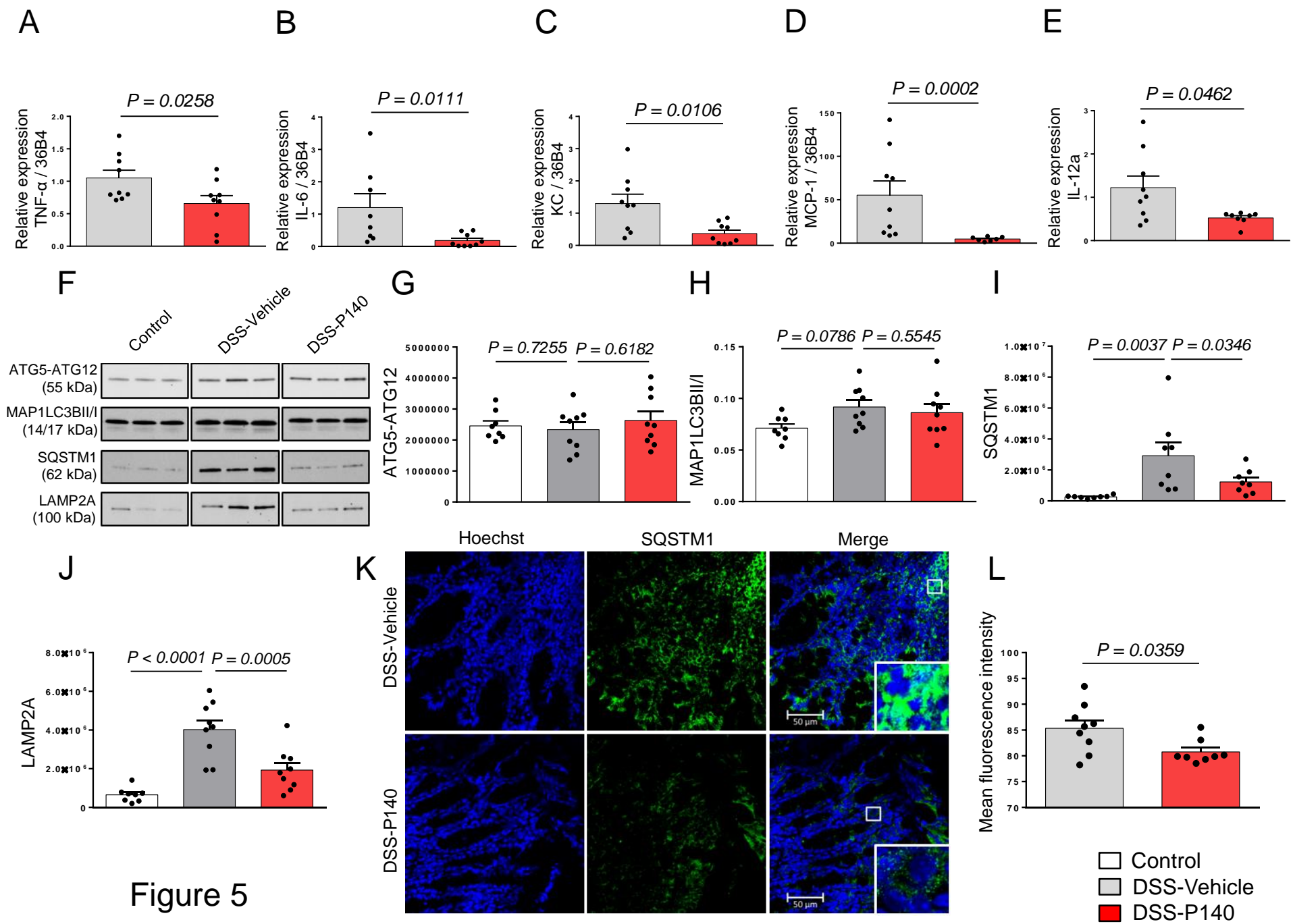


Figure 5